

Document downloaded from:

<http://hdl.handle.net/10251/92323>

This paper must be cited as:

Verdú Amat, S.; Vásquez, F.; Grau Meló, R.; Ivorra Martínez, E.; Sánchez Salmerón, AJ.; Barat Baviera, JM. (2016). Detection of adulterations with different grains in wheat products based on the hyperspectral image technique: The specific cases of flour and bread. *Food Control*. 62:373-380. doi:10.1016/j.foodcont.2015.11.002



The final publication is available at

<http://doi.org/10.1016/j.foodcont.2015.11.002>

Copyright Elsevier

Additional Information

Detection of adulterations with different grains in wheat products based on the hyperspectral image technique: the specific cases of flour and bread.

Samuel Verdú^{1*}, Francisco Vásquez³, Raúl Grau¹, Eugenio Ivorra², Antonio J. Sánchez², José M. Barat¹

¹Departamento de Tecnología de Alimentos. Universidad Politècnica de València, Spain.

²Departamento de Ingeniería de Sistemas y Automática, Universidad Politècnica de València, Spain

³Departamento de Tecnología de Alimentos de Origen Vegetal. Centro de Investigación en Alimentación y Desarrollo A,C, Hermosillo, Sonora, Mexico.

*Author for correspondence: Samuel Verdú

Address: Edificio 8G - Acceso F – Planta 0

Ciudad Politécnica de la Innovación

Universidad Politécnica de Valencia

Camino de Vera, s/n

46022 VALENCIA – SPAIN

E-mail: saveram@upvnet.upv.es

Phone: +34 646264839

Abstract

The objective of this study was to test the capability of a SW-NIR hyperspectral image technique to detect adulterations in wheat flour and bread with cheap grains, such as sorghum, oats and corn, and to compare the hyperspectral information with the physicochemical alterations in the properties of products. Wheat flour was adulterated at four different degrees (2.5, 5, 7.5 and 10%) with sorghum, oat and corn flours. Flours were prepared and used to make bread. Flours and breads were characterized according to several physicochemical parameters (pasting properties, water activity, mass loss during the baking process and texture profile analysis). Crumbs were extracted from breads and conditioned. Hyperspectral image captures were taken of both flours and conditioned crumbs. The data analysis was based on multivariate statistical process control method (MSPC), where the differentiation of adulterated samples was observed in all cases for both flours and crumbs. Finally, in order to relate the image analysis results and the adulterated sample properties, a correlation significance map was created between the physicochemical properties of samples and the multivariate statistical parameters. The SW-NIR image technique was capable of detecting adulterations in each case and high correlation significances were observed ($\alpha = 0.01$) between wavelengths from specific spectra zones and the physicochemical properties of samples.

Keywords: bread, adulteration, image analysis, MSPC, hyperspectral

1. Introduction

Adulteration of food products (raw materials, intermediate products, authorized additives, end products, etc.) is of primary concern for consumers, food processors, regulatory agencies and industries. Adulteration typically involves replacing or diluting high-cost ingredients with cheap low-quality products (Kalivas et al., 2014). The history of food adulteration reports not only economic motives, but even criminal ones. Thus food frauds and adulterations may have economic implications for local authorities due to increased work load and costs to governments through loss of value-added taxes made from sales (Tähkäpää, Maijala, Korkeala, & Nevas, 2015). Therefore, rapid qualitative analyses are required to separate adulterated samples, followed by a quantitative analysis of this adulterant, if necessary.

The development of non-destructive rapid analysis methods is an area in which interest increased a few years ago. Within this area, numerous methods based on different chemical and physical principles have been proposed to carry out both qualitative and quantitative determinations in laboratories and process chains. The methods which have demonstrated high versatility and robustness are those based on the simultaneous analysis of the large number of wavelengths of electromagnetic spectra, and in all their modes (reflectance, absorbance, interactance, etc.) (Wu & Sun, 2013). Specifically, the study of infrared spectra (IR) has been used for a vast number of determinations from multiple food matrices and analytes.

Two of the main techniques used for this purpose are IR spectroscopy and spectral imaging analysis. Several recent IR spectroscopy applications for detecting adulterations, fraud and contaminants have included the detection of pork adulteration in veal products based on FT-NIR spectroscopy (Schmutzler, Beganovic, Böhler, &

Huck, 2015), minced lamb meat adulteration (Kamruzzaman, Sun, ElMasry, & Allen, 2013), minced beef adulteration with turkey (Alamprese, Casale, Sinelli, Lanteri, & Casiraghi, 2013), fraudulent adulteration of chili powders with Sudan dye (Haughey, Galvin-King, Ho, Bell, & Elliott, 2014), adulteration of oil used in animal feed production (Graham et al., 2012), etc. Concretely, into the area of grain product adulterations, (Cocchi et al., 2006), developed a method to quantify the degree of adulteration of durum wheat flour with common bread wheat flour based on near-infrared spectroscopy assisted by different multivariate calibration techniques. Although fewer works have been carried out using the spectral imaging analysis technique, it has also been used in a large number of applications to detect adulteration of beef and pork in raw meats (Ropodi, Pavlidis, Mohareb, Panagou, & Nychas, 2015), melamine in milk powders (Fu et al., 2014), gelatin adulteration in prawn (Wu, Shi, He, Yu, & Bao, 2013), and for the pattern recognition for the categorization and authentication of red meat (Kamruzzaman, Barbin, Elmasry, Sun, & Allen, 2012), etc.

The objective of this work was to study the feasibility of an SW-NIR hyperspectral image technique to detect adulterations in wheat flour and bread with other cheap grains, such as sorghum, oat and corn, and to compare the hyperspectral information with the adulteration repercussions for flour and bread properties.

2. Material and Methods

2.1 Flour types and raw materials

The commercial wheat flour (WF) used was obtained from a local producer (Molí de Picó-Harinas Segura S.L. Valencia, Spain), whose chemical composition was:

12.7±0.6% of proteins, 1.0±0.03% of fat, 13.09±0.5% of moisture, and 0.32±0.1% of ash (w.b). The alveographic parameters were also facilitated by the company, which were $P = 94 \pm 2$ (maximum pressure (mm)), $L = 128 \pm 5$ (extensibility (mm)), $W = 392 \pm 11$ (strength (J-4)) and $P/L = 0.73$. Oat and corn flours were obtained from a local supermarket (La Carabasseta, Valencia, Spain). Their composition was 11.3±0.1% of proteins, 8.0±0.1% of fat, 12.6±0.6% of moisture and 0.92±0.1% of ash (w.b), and 8.3±0.1% of proteins, 2.8 ±0.1% of fat, 12.89±0.6% of moisture and 0.38±0.1% of ash (w.b), respectively. Sorghum flour was obtained from a commercial bakery (Integral Food S.A. Barcelona, Spain), whose composition was 10±0.1% of proteins, 1.7±0.5% of fat, 12.6±0.6% of moisture and 1.74±0.1% of ash (w.b). In order to maintain particle size homogeneity, grain flours were analyzed and remilled in a stainless steel grinder, whenever necessary (Retsch GmbH, ZM 200, Haan, Germany), until particle size distribution with no significant differences was achieved with the wheat flour used. The particle size of flours was measured 6 times by laser scattering in a Mastersizer 2000 (Malvern, Instruments, UK), equipped with a Scirocco dry powder unit. The results were expressed as a maximum size in μm at 10%, 50% and 90% (d (0.1), d (0.5) and d (0.9), respectively) of the total volume of the analyzed particles as their averages (D [4, 3]). The average results were $d (0.1) = 25.5 \pm 1.1$, $d (0.5) = 92.0 \pm 0.6$, $d (0.9) = 180.6 \pm 0.8$ and $D [4, 3] = 99.4 \pm 1.2$. Having ensured homogeneous particle size, in order to simulate possible adulterations, binary mixes were made by adding different percentages of sorghum, oat or corn to wheat flour. Specifically, adulterations were 2.5, 5, 7.5 and 10% (w/w) of wheat flour with all the different flour grain types.

The other ingredients to make bread were sunflower oil (maximum acidity 0.2° Koipesol Semillas, S.L., Spain), pressed yeast (*Saccharomyces cerevisiae*, Lesafre Ibérica, S.A., Spain), white sugar ($\geq 99.8\%$ of saccharose, Azucarera Ebro, S.L., Spain)

and salt (refined marine salt $\geq 97\%$ NaCl Salinera Española S.A., Spain), which were purchased in local stores.

2.2 Bread-making process

The formulation used to prepare bread dough was based on previous works (Verdú, Vásquez, et al., 2015) and was as follows: 56% flour (pure wheat flour or the adulterated versions), 2% refined sunflower oil, 2% commercial pressed yeast, 4% white sugar 1.5% salt and 34.5% water. The process was carried out by mixing all the ingredients in a food mixer (Thermomix® TM31, Vorwerk, Germany) according to the following method: in the first phase, liquid components (water and oil), sugar and salt were mixed for 4 minutes at 37 °C. Pressed yeast was added in the next phase to be mixed at the same temperature for 30 seconds. Finally, flour was added and mixed with the other ingredients according to a default bread dough mixing program, which makes homogeneous dough. The program system centers on mixing ingredients with random turns of the mixer helix in both directions (550 revolutions/minute) to obtain homogeneous dough. This process was applied for 4.5 minutes at 37 °C. Then 450 g of dough were placed in the metal mold (8x8x30cm) for fermentation. Height was approximately 1 cm.

Dough fermentation was carried out in a chamber with controlled humidity and temperature (KBF720, Binder, Tuttlingen, Germany). The fermentation process conditions were 37 °C and 90% relative humidity (RH). Samples were fermented for 1 h. The baking process was carried out at the end of fermentation. Metal molds were placed in the middle of the oven (530x450x340, grill power 1200W, internal volume

32L, Rotisserie, DeLonghi, Italy) plate, which was preheated to 180 °C. Baking time was 35 minutes.

2.3 Crumb conditioning

Having baked the breads, crumbs were extracted and processed to be analyzed as so: crumbs from central bread zones (the middle third of total bread length) were removed from the crust and dried in a food dryer (Excalibur 3900B Deluxe Dehydrator) at 50 °C to obtain the same moisture of raw flours (approx. 13% of moisture). Dried crumbs were milled in a stainless steel grinder (Retsch GmbH, ZM 200, Haan, Germany) until particle size distribution with no significant differences was achieved with the flours used.

2.4 SW-NIR data acquisition and processing

Images of both groups of samples (flours and crumbs from pure wheat and adulterated versions) were taken with a Photonfocus CMOS camera, model MV1-D1312 40gb 12 (Photonfocus AG, Lachen, Switzerland), and using a SpecimImSpector V10 1/2" filter (Specim Spectral Imaging, LTD., Oulu, Finland), which works as a linear hyperspectral camera. The illuminant was an ASD illuminator reflectance lamp (ASD Inc, Boulder, USA), which produces stable illumination over the full working spectral range. Fifteen grams of sample were placed into a glass Petri dish (10 cm diameter) and a homogeneous surface and height were maintained (approx. 0.75 cm). Spectra were collected directly at room temperature. Four samples of each flour, mix and crumb flours were prepared. Five images of each were acquired by rotating 1.04 radians each time around its normal axis. Twenty image acquisitions of each case were obtained. The

position of the illuminant and camera in relation to the sample was always constant in order to control lighting conditions and to obtain a constant image size. In order to avoid any heat transfer to the sample, the distance between the illuminant and the sample was 0.5 m. The distance between the camera and the sample was 0.15 m. The obtained image (scanned line) comprised 256 gray levels (8 bits). The diffuse reflectance spectrum was collected with 53 different wavelengths (each wavelength was digitalized with 8 bits). These wavelengths were distributed at intervals of 11.2 nm within the 400-1000 nm range. The scanned line comprised 1312 points, so an image was recorded with a resolution of 1312 x 1082 pixels. Image reflectance calibration and preprocessing were performed as described in (Verdú, Ivorra, Sánchez, Barat, & Grau, 2015). The camera was operated by a software, developed based on SDK Photonfocus-GigE_Tools, and programming language C++ was used.

2.3 Physico-chemical parameters

2.3.1 Pasting properties of flours

For the purpose of evaluating the influence of different adulterations on flours, pasting properties were analyzed using the viscosity profile obtained by the RVA (Rapid Visco Analyser Super 4, Newport Scientific) viscometer. To this end, the method was approved by the AACC (America Association of Cereal Chemists), whose reference is the “General Pasting Method for Wheat or Rye Flour of Starch Using the RVA. AACC 2000 number 76-21” was used. Samples of $3 \text{ g} \pm 0.01 \text{ g}$ were weighed and $25 \text{ g} \pm 0.01 \text{ g}$ of water were incorporated. The test started at 50 °C and 960 RPM, and was then slowed down to 160 RPM at 10 s. Temperature was maintained during the first minute, and went from 50 °C to 95 °C to then increase during the next 4 minutes to reach 95 °C at

minute 5 in a second step. The third step involved maintaining the temperature at 95 °C until minute 7.5. The fourth step was to lower the temperature to 50 °C, which was reached at minute 11. The last step entailed maintaining a temperature of 50 °C until minute 13. Measurements were taken in triplicate. The obtained pasting parameters were pasting temperature (T_p), peak viscosity (P_v), trough viscosity (T_v), breakdown viscosity (B_v), final viscosity (F_v), setback viscosity (S_v) and peak time (P_t).

2.3.2 Baking loss, water activity and texture profile analysis of breads

To evaluate the effect of adulteration on the end product, some of most relevant bread properties were studied. In this phase, mass loss during the baking process (ΔM_b) was concluded by the difference between the pre-baking dough weight and the finished bread weight (both bread products were cooled at room temperature for 1 h). This parameter was called “baking loss”. The water activity of raw crumbs (a_w) was determined in an Aqualab® dew point hygrometer (DECAGÓN Aqualab CX-2, Pullman, WA, USA). The texture profile analysis (TPA) was performed following the method used by [1], where two 12.5-mm-thick cross-sectional slices were obtained from the center of each bread product. The texture profile analysis was carried out in a TA-TX2 texture analyzer (Stable Micro Systems, Surrey, UK). A 25-kg load cell (35-mm diameter) was used. The assay speed was set at 1.7 mm/s to compress the bread crumb center at 50% of its previous height. The time between compressions was 5 s. The studied parameters were hardness (D), springiness (S), cohesiveness (C), gumminess (G), chewiness (Ch) and resilience (R).

2.4 Statistical analysis

The study of the hyperspectral results was based on Multivariate Statistical Process Control (MSPC). This method derives from the Univariate Control Process, and offers the possibility of including a large number of variables and the interactions among them at the same time. The objective of MSPC is to create a model based on the required features of samples and the generation of thresholds (confidence limit), which determines the conformity of new samples according to the pre-established specifications (normal conditions) to then maintain the system under control (Bersimis, Psarakis, & Panaretos, 2007). The process can be used by including new multivariate data in the created model, and evaluating the distance of any new samples from the model by studying T^2 -statistic (Hotelling's), and Q-statistic (Q-residuals). The situation of these parameters within the confidence limit indicates samples according to the pre-established requirements, and then under control (samples of pure wheat flour and pure wheat flour breads). On the contrary, any samples situated beyond the confidence limits imply that something occurred under the controlled conditions which caused a deviation from the model (adulterated samples, if applicable). Any T^2 -statistic beyond the control is interpreted as both new samples that present an unusual distance from the center of the model, and alterations in the values of some of their variables. Any Q-statistic beyond the control represents samples that the model is incapable of describing, which means the presence of some irregularities in the control variables that first allow the identification and then separation from the samples under the control.

The physicochemical parameters obtained from flours (T_p , P_v , T_v , B_v , F_v , S_v , P_t) and breads (ΔM_b , a_w and TPA (H , S , C , G , Ch)) were studied by a one-way variance study (ANOVA). In those cases in which the effect was significant (P -value < 0.05), means were compared with Fisher's least significant difference (LSD) procedure.

Procedures were performed with PLS Toolbox, 6.3 (Eigenvector Research Inc., Wenatchee, Washington, USA), a toolbox extension in the Matlab 7.6 computational environment (The Mathworks, Natick, Massachusetts, USA).

3. Results

3.1 MSPC results

Figure 1 provides the MSPC statistical analysis results in Q-residuals terms applied to spectra data. This statistic was used to observe the capability of the created models (based on pure wheat flour and pure wheat flour bread crumbs) to place the adulterated samples beyond the confidence limit. Both the flours and adulterated bread crumbs were located beyond the 95% confidence limit of their respective pure wheat models, regardless of the cereal type used for adulteration and percentage. The percentage of adulteration revealed evolution across the Q-residuals axis following the degree, where the cases with 2.5% came close to the limit, while those with 10% were the most distant ones. Of the adulterated flours, sorghum and corn presented a clear differentiation among the obtained adulteration percentages, but oat showed more agglomeration in its points. The behavior of crumbs was the same as the adulteration degree, but cereal type appeared to have an influence. Crumbs from the breads adulterated with sorghum remained well beyond the model limit in all cases, with even a wider separation compared to its analog flour, and the same occurred with oat, but its position was closer to the limit compared to sorghum. Crumbs from the bread adulterated with corn showed more differences compared to their analog flours. The degrees of 2.5% and 5% came into contact with the limit line, and even caused problems for detecting some samples.

Then the baking process influenced the response of the hyperspectral technique. Sorghum and oat presented minor differences between the flour and crumb results, but

the bread-making process apparently made it difficult to detect corn in some bread crumbs at low adulteration percentages, although corn was detected in most samples.

The results showed that the used technique has reached a detection sensibility until 2.5% of adulteration for all grains. In early works, durum wheat flour adulterated with soft wheat flour was detected with a sensibility of 0.5% using NIR spectroscopy (Cocchi et al., 2006). In the same way, detection of soft wheat had also been addressed using other methods as the determination of alkylresorcinol composition in pasta, obtaining a sensibility of 5% (Knödler, Most, Schieber, & Carle, 2010), as well as DNA microsatellite region method, where until 1% of adulteration was detected in durum wheat semolina, pasta and bread (Sonnante et al., 2009). Moreover, adulterations with other flours have been detected at 0.1%, concretely in the case of lupin seed flour, by real-time PCR method (Scarafoni, Ronchi, & Duranti, 2009). In comparison to works reported previously, the sensibility of the present method is within high intermediate place, taking into account that it was configured as online inspection tool.

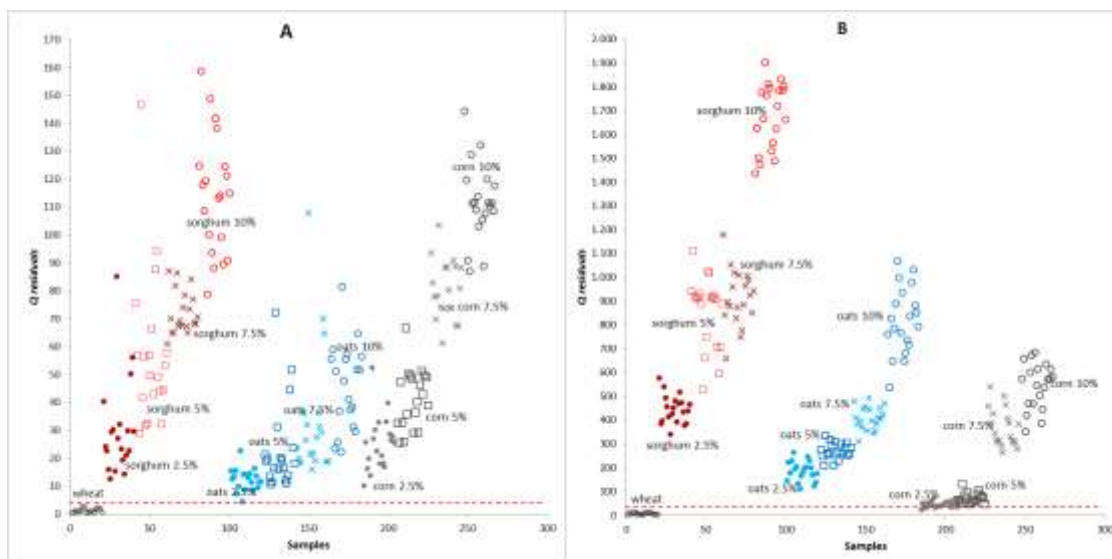


Figure 1. The Q-residuals results for adulterated flour samples (A) and crumb samples (B). The dashed horizontal red line indicates a 95% confidence limit. Red corresponds to sorghum, blue to oat, gray to corn and black to wheat. The series of shapes are arranged according to the percentage of adulteration: ● 2.5%, □ 5%, × 7.5% and ○ 10%.

To study the exclusion process of adulterated samples, the Q-contributions of each variable (wavelength) per sample were compared. The Q-contribution plots report information about the causes of the disturbance to the process in terms of the original variables' influence. A high absolute Q-contribution value for a given variable means a problem with that specific variable (Westerhuis, Gurden, & Smilde, 2000). Figure 2 shows the plotted mean results of the Q-contributions based on each adulteration of cereal. The Q-contributions for the pure flours of sorghum, oat and corn were included in the adulterated flours plots to compare their results with the adulterated wheat flour and their main peaks within the spectra. First, a main peak across spectra appeared in both the visible and the infrared zones for all the cereal types. Flours presented an increment in contributions following the increase in the degree of adulteration for all the cereals (Figure 2 (left plots)), which brought about the most marked peaks for sorghum, while corn obtained the least marked one. There were common spectra zones with high

values for all the cereals, but with different intensities. The corresponding variables of these peaks were wavelengths 490, 556, 612, 792 and 904 nm for sorghum and oat. Corn presented the same wavelengths, but by adding 859 nm and removing 612 nm.

For the crumb results (Figure 2 (right plots)), the degrees of adulteration also followed the position order in the plot. Peaks presented differences in regard to flours. In this case, the common variables with a heavy weight were wavelengths 523, 747, 848, 926 and 948 nm. In the same way as flours, sorghum presented the most marked peaks and corn the least marked one. However, wavelength 814 showed the inverse behavior as it achieved considerable importance for oat and corn.

Although the fundamental composition of the adulterated flours and crumbs was the same, the bread-making process influenced the response of the hyperspectral image device.

3.2 Repercussions of adulteration on flour and bread properties, and its relationship with hyperspectral detection

Adulteration can be detected by the hyperspectral image technique. Nevertheless, in order to ensure that the observed statistical results were related to the real effect of adulteration on the product, and was not produced by any uncontrolled factor, some physicochemical properties of both flours and breads were tested and related with the MSPC results.

First, a battery of physicochemical analyses was carried out to characterize pure wheat flour and bread, and their adulterated versions with the different cereals. On the one hand, flours were characterized according to their pasting properties with the RVA. On

the other hand, whole breads were analyzed in terms of baking loss, water activity and texture properties based on the TPA. Table 1 contains the physicochemical analysis results.

Table 1. Results of the physicochemical characterization of flours and breads

Cereal	%adulteration	Flours							Breads							
		Tp	Pv	Tv	Bv	Fv	Sv	Pt	ΔM_b	a_w	D	S	C	G	Ch	R
Wheat flour	0	68.9±0.6a	2245±15a	1421±4a	823±10a	2660±5a	1238±10a	6.1±0.2a	33.5±3.5a	0.955±0.003a	9.3±0.1a	0.98±0.04 a	0.81±0.01a	7.5±0.7a	7.4±0.8a	0.44±0.01a
Sorghum	2.5	68.9±0.5a	2164±7a	1308±48a	856±26b	2614±58a	1306±10b	6.04±0.05 a	36.1±2.8a	0.956±0.003b	8.2±0.1a	0.98±0.02 a	0.80±0.01b	6.5±0.8a	6.4±0.9a	0.43±0.01a
	5	87.2±0.1b	2225±19b	1369±7b	856.5±26b	2742±6b	1373±13c	6.13±0.01a	37.2±2.5ab	0.958±0.003b	9.3±0.2a	0.96±0.04 a	0.79±0.01b	7.4±0.7a	7.2±0.9a	0.43±0.01 a
	7.5	87.2±0.1b	2214±18b	1339±12b	875±5bc	2833±6c	1494±19d	6±0.04a	38.2±3.7b	0.959±0.003c	9.6±1.4a	0.98±0.02a	0.80±0.01b	7.7±1.1a	7.6±1.0a	0.44±0.01 a
	10	87.±0.5b	2306±199c	1422±7b	884±26c	3029±47d	1607±54e	6.07±0.09a	38.6±4b	0.960±0.002c	10.5±1.5a	0.97±0.03a	0.78±0.07b	8.2±1.1a	8.0±1.1a	0.43±0.01 a
Oats	2.5	69.3±1.1a	2194±26a	1396.5±37a	798±11a	2564±54a	1168±16a	6.17±0.05a	38.3±2.9b	0.957±0.002a	6.3±1.0b	0.94±0.07a	0.82±0.01ab	5.2±0.8b	4.9±0.9b	0.45±0.01ab
	5	70.18±0.1a	2245±31a	1426±9a	819±41a	2658±45a	1232±55a	6.17±0.05a	38.8±3.2b	0.961±0.008a	6.7±0.7b	0.98±0.01a	0.82±0.01b	5.5±0.6b	5.4±0.6b	0.45±0.01ab
	7.5	84.73±0.1b	2246±44a	1429±45a	817±1a	2675±25a	1246±19a	6.14±0.09a	37.8±3.5b	0.961±0.001c	6.1±0.9b	0.97±0.08a	0.82±0.01b	5.0±0.7b	4.9±1.0b	0.45±0.01ab
	10	85.15±0.1b	2266±12a	1476±36a	790±24a	2715±14a	1239±22a	6.2±0.1b	39.2±0.7b	0.969±0.002d	4.8±1.0c	0.92±0.11a	0.83±0.01b	4.0±0.8c	3.7±0.9c	0.45±0.01b
Corn	2.5	69.33±0.1a	2210±10a	1363.5±14a	847±4b	2577±26a	1214±11a	6.07±0.01b	37.9±3.6ab	0.957±0.008a	7.2±0.1b	0.96±0.04a	0.81±0.01a	5.9±0.5a	5.7±0.6b	0.44±0.01ab
	5	85.95±0.1b	2219±14a	1374.5±7b	844±21b	2651±12a	1277±19b	6.04±0.05c	38.2±1.6b	0.960±0.002a	5.2±1.1c	0.95±0.05a	0.83±0.01ab	4.3±0.8b	4.1±0.9b	0.45±0.01 ab
	7.5	85.15±0.5b	2201.5±31a	1374±35b	867±3c	2669±44a	1335±9c	5.93±0.02d	40.2±2bc	0.960±0.002a	4.7±1.3c	0.94±0.07a	0.84±0.01ab	4.0±1.0b	3.8±1.1b	0.45±0.01ab
	10	84.83±0.4b	2260±14a	1379.5±24b	890±10d	2728±25b	1358.5±50d	5.97±0.14d	40.4±1.1c	0.966±0.005b	5.6±0.8c	0.95±0.05a	0.85±0.05b	4.8±0.6b	4.6±0.7b	0.45±0.01b

Tp: pasting temperature, Pv: peak viscosity, Tv: trough viscosity, Bv: breakdown viscosity, Fv: final viscosity, Sv: setback viscosity, Pt: peak time. ΔM_b : baking loss, a_w : water activity, D: hardness, S: springiness, C: cohesiveness, G: gumminess, Ch: chewiness, R: resilience. Letters in columns mean significant differences at a p-value < 0.05 of each adulteration cereal compared only to wheat flour.

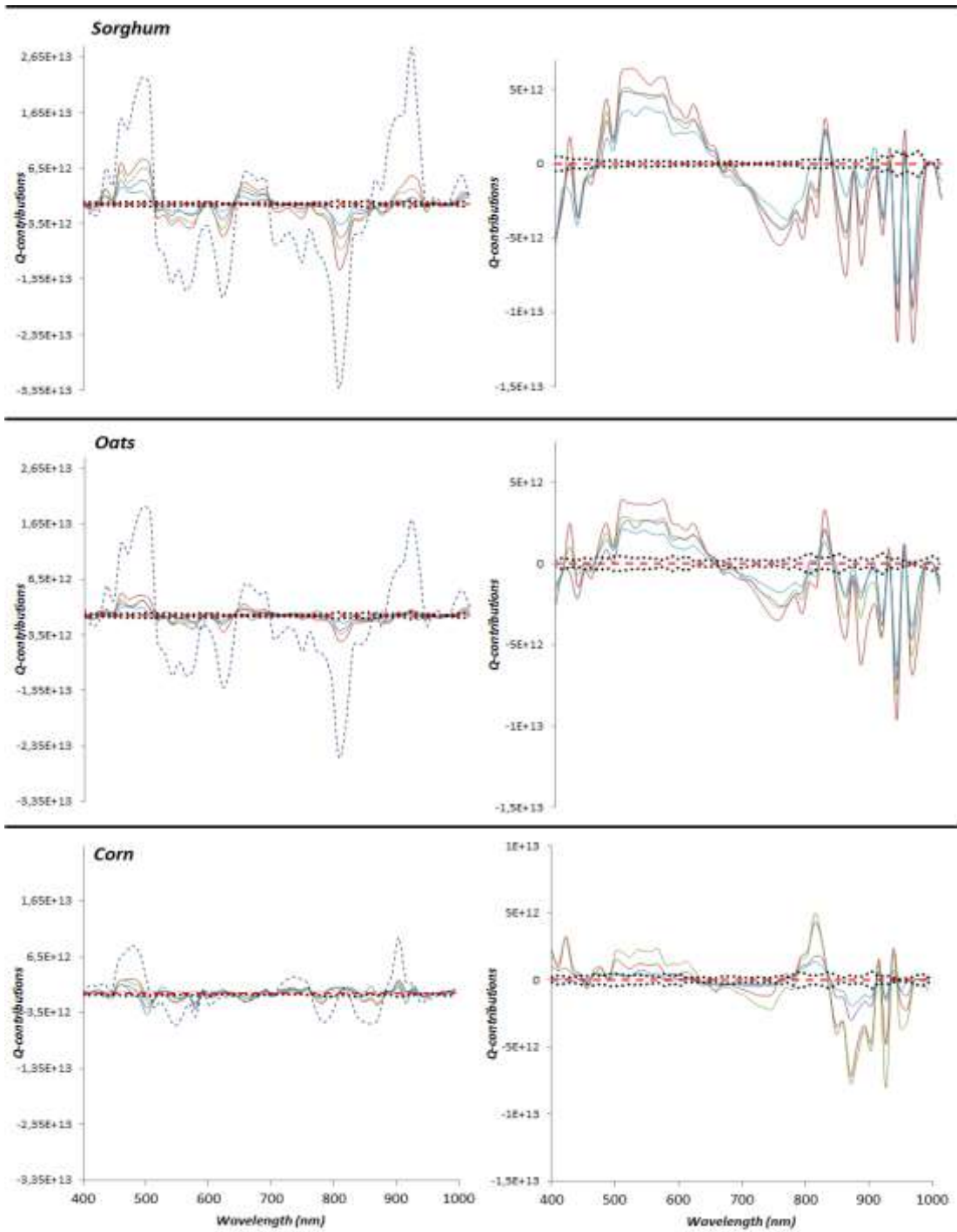


Figure 2. The Q-contributions plots for the adulterated flours (left) and crumbs (right) for each cereal. The dashed red lines represent pure wheat, while the dashed black lines denote the standard deviation of the pure wheat contributions. The dashed blue lines correspond to pure cereal flour adulteration. The red line indicates 10% of adulteration, the green line corresponds to 7.5%, the purple line to 5% and the blue line to 2.5%.

The physicochemical analysis results verified the influence of degree of adulteration and the type of cereal used. The effects of pasting properties led to differences depending on the cereal used. In general terms, some pasting properties, e.g. pasting temperature, was affected by them all from 7.5% of adulteration, and even from 5% for sorghum and corn. Some properties had no influence in any case, such as peak viscosity, breakdown viscosity or setback for oat. Breads also presented significant modifications to ΔM_b , a_w and to some textural properties, such as hardness and cohesiveness. However, some textural properties were not affected by any cereal or degree of adulteration, such as springiness.

Having collected the information about the physicochemical properties of samples, a study of whether these results agreed with the previously observed hyperspectral results was conducted. Here the objective was not to find dependencies between hyperspectral data and physicochemical properties to develop a prediction model, but to ensure that the imaging analysis response was in accordance with the measurable influence of adulteration on products. For this purpose, a correlation coefficient was calculated between the Q-contribution values from all the wavelengths and the studied physicochemical variables of flours and breads for each degree of adulteration. By way of example, Figure 3 shows the correlation of several variables from flours and breads for the Q-contributions of the wavelengths for sorghum adulteration. The correlation level differed for each variable. Setback viscosity (Sv) and pasting temperature (Tp) maintained a similar correlation level for each wavelength, and setback viscosity was slightly high. Although peak viscosity (Pv) tended to obtain a high correlation coefficient at the same wavelengths, it presented a high or equal correlation at the 0.80 level in only a few cases (Figure 3-A). Bread variables also exhibited irregular behavior, where the same peaks and zones with the maximum correlation level across the spectra

for baking loss (ΔMb) and water activity (a_w) were observed, while hardness (D) presented quite less peaks above the 0.80 level (Figure 3-B).

The results showed that the hyperspectral information indeed was influenced by the variations caused by the adulteration effects. In order to ensure the observed relationships, a decision was made to determine the degree of significance for each correlation. The results were studied at three degrees of significance ($\alpha=0.05$, $\alpha=0.025$ and $\alpha=0.01$) based on the t-statistic. Figure 3-C and 3-D graphically depict the results of the level of significance for the physicochemical variables used as an example of sorghum adulteration (Figure 3-A and 3-B). We can see how the significance of the correlations presented variability for the coefficients that presented no differences.

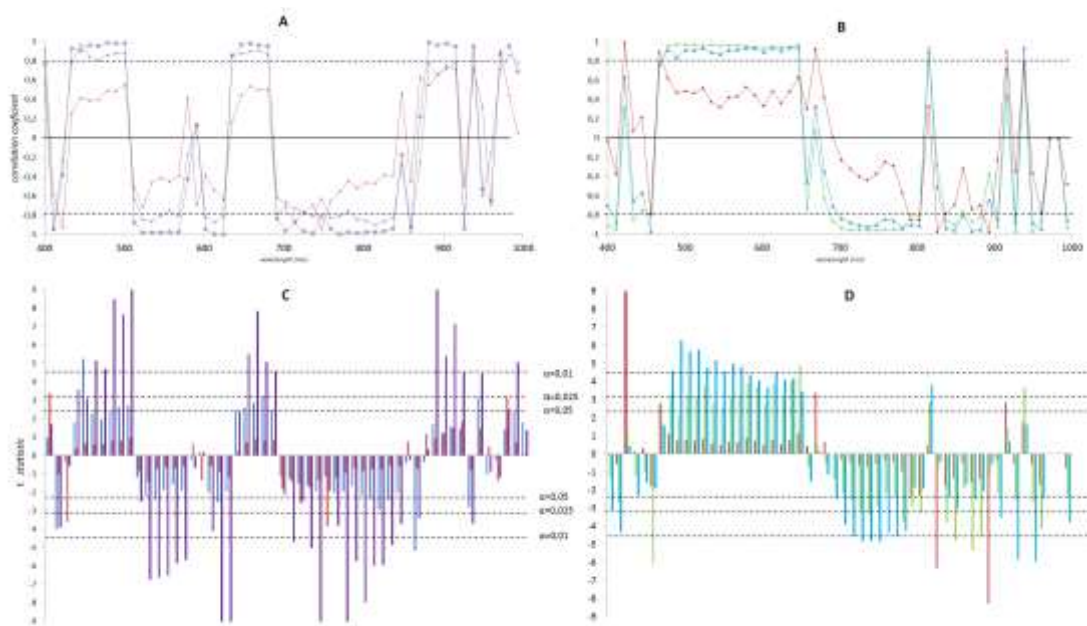


Figure 3. The correlation coefficient spectra between the Q-contributions of each wavelength and some physicochemical parameters of flour (A) and bread (B) adulterated with sorghum flour; Tp: pasting temperature, Pv: peak viscosity, Sv: setback viscosity, ΔMb : baking loss, a_w : water activity, D: hardness. The dashed black line in A and B marks the positive and negative threshold for the correlation level = 0.80. Lower images (C and D) represent the level of significance based on the t-statistic test for each correlation coefficient of the previous correlations. The dashed black lines represent confidence levels of 95, 97.5 and 99%.

This procedure was carried out for each cereal and physicochemical variable to obtain a correlation significances map and to observe the differences among them. Table 2 shows a map of the level of significance map for correlation according to the gray tones.

The correlation results influenced cereal type and whether the analyzed matrix was flour or bread from the same degree of adulteration. With flours, the cereal with higher correlations, and at the same time, higher correlation significances at the 99% confidence level, was sorghum, followed by corn and oats, and presented fewer significant correlations. With breads, the adulteration with oats presented the highest correlation levels of significance, followed by sorghum and corn. In general, the common correlations observed for the pasting properties of all the adulterated flours lay inside the visible and infrared zones. The common visible wavelengths zones were around 422, 467 and 523 nm, while the infrared wavelengths zones were about 724-792, 860-915 and 982 nm. Breads also presented common zones within the visible and infrared zones. Specifically, 411, 456-478, 501-568 nm for the visible and the infrared zones presented almost all the wavelengths from 700 to 980.

Not all the physicochemical variables and cereal types had the same number of high correlations with spectra, although the results sufficed to conclude that the relationship between the hyperspectral data and the physicochemical data was observed. This means that the recognized pattern based on MSCP was produced neither randomly nor by uncontrolled factors, but was due to the influence of the adulteration levels on products.

5. Conclusions

The capability of the hyperspectral imaging technique used herein to detect adulterations in the tested products at the proposed levels was successful. The bread-making process did not affect detection, but could generate false-negatives in low adulteration percentages in bread with corn. Sorghum was the least affected by this process. The relationship between the hyperspectral data and the physicochemical data indicated that detection was actually based on the modifications produced by adulteration. The results proved that a tool based on this principle could be useful for detecting adulterations of this type. Experiments that include more grain types and other flour products would be interesting to help advance in developing a plausible inspection tool.



Figure 4. Correlation map. Gray marks the correlation's level of significance: 95%, 97.5%, 99%. The positions in white indicate a non-significant correlation. Tp: pasting temperature, Pv: peak viscosity, Tv: trough viscosity, Bv: breakdown viscosity, Fv: final viscosity, Sv: setback viscosity, Pt: peak time. ΔMb: baking loss, aw: water activity, D: hardness, S: springiness, C: cohesiveness, G: gumminess, Ch: chewiness, R: resilience.

6. Bibliography

- Alamprese, C., Casale, M., Sinelli, N., Lanteri, S., & Casiraghi, E. (2013). Detection of minced beef adulteration with turkey meat by UV-vis, NIR and MIR spectroscopy. *LWT - Food Science and Technology*, *53*, 225–232. doi:10.1016/j.lwt.2013.01.027
- Bersimis, S., Psarakis, S., & Panaretos, J. (2007). Multivariate statistical process control charts: An overview. *Quality and Reliability Engineering International*. doi:10.1002/qre.829
- Cocchi, M., Durante, C., Foca, G., Marchetti, A., Tassi, L., & Ulrici, A. (2006). Durum wheat adulteration detection by NIR spectroscopy multivariate calibration. *Talanta*, *68*, 1505–1511. doi:10.1016/j.talanta.2005.08.005
- Fu, X., Kim, M. S., Chao, K., Qin, J., Lim, J., Lee, H., ... Ying, Y. (2014). Detection of melamine in milk powders based on NIR hyperspectral imaging and spectral similarity analyses. *Journal of Food Engineering*, *124*, 97–104. doi:10.1016/j.jfoodeng.2013.09.023
- Graham, S. F., Haughey, S. A., Ervin, R. M., Cancouët, E., Bell, S., & Elliott, C. T. (2012). The application of near-infrared (NIR) and Raman spectroscopy to detect adulteration of oil used in animal feed production. *Food Chemistry*, *132*, 1614–1619. doi:10.1016/j.foodchem.2011.11.136
- Haughey, S. A., Galvin-King, P., Ho, Y. C., Bell, S. E. J., & Elliott, C. T. (2014). The feasibility of using near infrared and Raman spectroscopic techniques to detect fraudulent adulteration of chili powders with Sudan dye. *Food Control*. doi:10.1016/j.foodcont.2014.03.047
- Kalivas, J. H., Georgiou, C. A., Moira, M., Tsafaras, I., Petrakis, E. A., & Mousdis, G. A. (2014). Food adulteration analysis without laboratory prepared or determined reference food adulterant values. *Food Chemistry*, *148*, 289–293. doi:10.1016/j.foodchem.2013.10.065
- Kamruzzaman, M., Barbin, D., Elmasry, G., Sun, D. W., & Allen, P. (2012). Potential of hyperspectral imaging and pattern recognition for categorization and authentication of red meat. *Innovative Food Science and Emerging Technologies*, *16*, 316–325. doi:10.1016/j.ifset.2012.07.007
- Kamruzzaman, M., Sun, D. W., ElMasry, G., & Allen, P. (2013). Fast detection and visualization of minced lamb meat adulteration using NIR hyperspectral imaging and multivariate image analysis. *Talanta*, *103*, 130–136. doi:10.1016/j.talanta.2012.10.020
- Knödler, M., Most, M., Schieber, A., & Carle, R. (2010). A novel approach to authenticity control of whole grain durum wheat (*Triticum durum* Desf.) flour and pasta, based on analysis of alkylresorcinol composition. *Food Chemistry*, *118*, 177–181. doi:10.1016/j.foodchem.2009.04.080
- Miñarro, B., Albanell, E., Aguilar, N., Guamis, B., & Capellas, M. (2012). Effect of legume flours on baking characteristics of gluten-free bread. *Journal of Cereal Science*, *56*(2), 476–481. doi:10.1016/j.jcs.2012.04.012

- Ropodi, a. I., Pavlidis, D. E., Mohareb, F., Panagou, E. Z., & Nychas, G.-J. E. (2015). Multispectral image analysis approach to detect adulteration of beef and pork in raw meats. *Food Research International*, *67*, 12–18. doi:10.1016/j.foodres.2014.10.032
- Scarafoni, a., Ronchi, a., & Duranti, M. (2009). A real-time PCR method for the detection and quantification of lupin flour in wheat flour-based matrices. *Food Chemistry*, *115*(3), 1088–1093. doi:10.1016/j.foodchem.2008.12.087
- Schmutzler, M., Beganovic, A., Böhler, G., & Huck, C. W. (2015). Methods for detection of pork adulteration in veal product based on FT-NIR spectroscopy for laboratory, industrial and on-site analysis. *Food Control*, *57*, 258–267. doi:10.1016/j.foodcont.2015.04.019
- Sonnante, G., Montemurro, C., Morgese, A., Sabetta, W., Blanco, A., & Pasqualone, A. (2009). DNA Microsatellite Region for a Reliable Quantification of Soft Wheat Adulteration in Durum Wheat-Based Foodstuffs by Real-Time PCR. *Journal of Agricultural and Food Chemistry*, *57*(21), 10199–10204. doi:10.1021/jf902624z
- Tähkääpää, S., Maijala, R., Korkeala, H., & Nevas, M. (2015). Patterns of food frauds and adulterations reported in the EU rapid alarm system for food and feed and in Finland. *Food Control*, *47*, 175–184. doi:10.1016/j.foodcont.2014.07.007
- Verdú, S., Ivorra, E., Sánchez, A. J., Barat, J. M., & Grau, R. (2015). Study of high strength wheat flours considering their physicochemical and rheological characterisation as well as fermentation capacity using SW-NIR imaging. *Journal of Cereal Science*, *62*, 31–37. doi:10.1016/j.jcs.2014.11.002
- Verdú, S., Vásquez, F., Ivorra, E., Sánchez, A. J., Barat, J. M., & Grau, R. (2015). Physicochemical effects of chia (*Salvia Hispanica*) seed flour on each wheat bread-making process phase and product storage. *Journal of Cereal Science*, *65*, 67–73. doi:10.1016/j.jcs.2015.05.011
- Westerhuis, J. A., Gurden, S. P., & Smilde, A. K. (2000). Standardized Q-statistic for improved sensitivity in the monitoring of residuals in MSPC. *Journal of Chemometrics*, *14*, 335–349. doi:10.1002/1099-128X(200007/08)14:4<335::AID-CEM579>3.0.CO;2-F
- Wu, D., Shi, H., He, Y., Yu, X., & Bao, Y. (2013). Potential of hyperspectral imaging and multivariate analysis for rapid and non-invasive detection of gelatin adulteration in prawn. *Journal of Food Engineering*, *119*, 680–686. doi:10.1016/j.jfoodeng.2013.06.039
- Wu, D., & Sun, D.-W. (2013). Advanced applications of hyperspectral imaging technology for food quality and safety analysis and assessment: A review — Part I: Fundamentals. *Innovative Food Science & Emerging Technologies*, *19*, 1–14. doi:10.1016/j.ifset.2013.04.014